Design and fabrication of micro-structured waveguides in nonlinear crystals

Mykhaylo Dubov[1], and Sonia Boscolo[1]
[1]*Aston Institute of Photonic Technologies, School of Engineering and Applied Science, Aston University, Birmingham B4 7ET, United Kingdom*
[*]*Corresponding author: s.a.boscolo@aston.ac.uk*

ABSTRACT
We review our recent work on design and fabrication of microstructured waveguides (WG) in birefringent nonlinear crystal, z-cut lithium niobate ($LiNbO_3$), and describe simulation approaches to both design and optimisation of such structures. We also review our experimental results achieved by using direct fs laser inscription in such hosts using high repetition rate femtosecond oscillator system. Refractive index (RI) contrasts as high as -0.0127 have been demonstrated for individual tracks. The experimental relations between RI contrast and track dimensions were used for optimisation of depressed cladding waveguides in such hosts. We demonstrate that the spectral range for such microstructured waveguides in $LiNbO_3$ can be extended up to the long-wavelength end of the transparency of material.
Keywords: lithium niobate, direct femtosecond laser microfabrication, microstructured anisotropic waveguide.

1. INTRODUCTION
The combination of excellent nonlinear ($\chi^{(2)}$) optical, electro-optical, acousto-optical and other properties, as well as its wide transparency range, make lithium niobate (LiNbO3) an attractive host material for applications in integrated nonlinear optics [1]. The majority of nonlinear optics applications require manufacturing of optical waveguides (WGs) to confine light propagation in reduced volumes, thus reaching high light intensities. As one of the most efficient techniques for three-dimensional volume micro-structuring of transparent dielectrics, the direct femtosecond (fs) laser inscription method [2, 3] has been widely applied to fabricate optical WGs in numerous optical materials, including optical crystals [4-6], ceramics [7, 8], glasses [9-12] and polymers [13,14]. The possibility of inscribing arbitrarily shaped WGs in the bulk of various crystals has allowed for new geometrical degrees of freedom in the design of integrated optical devices. Buried integrated laser sources, nonlinear-frequency converters, amplifiers, single-photon detectors and other devices have already been achieved based on this technology. While a transparent dielectric being irradiated by fs laser pulses, with the energy above certain threshold becomes absorbing, this occurs only in the vicinity of the focal point. This fact allows precision modification of the material refractive index (RI) by translating the sample continuously along a certain 3D path. Such a procedure can lead to the creation of isolated air holes or voids, periodic RI modulation or sometimes pearl chains and also continuous, smooth tracks that are suitable for low-loss light guiding [10]. The positive RI contrasts between exposed and unexposed areas that are typically induced by direct fs writing in optical glasses can be up to an order of magnitude higher than those of optical fibres. Continuous, smooth tracks can also be inscribed in various crystal materials, featuring reduced RI in the central area of the track [15] and slightly increased RI in the surrounding region. Single tracks in crystals may exhibit weak guiding, but it occurs only in the surrounding areas of the residual stress left within the material by the laser beam passage. On the other hand, by writing multiple tracks with a reduced RI around the unmodified volume of material it is possible to produce a 'depressed-index cladding' [4, 5] with the central (unmodified) volume serving as the core of WG, whereby the mechanical stress has only minor influence on the WG modes. The simplest type of depressed-index cladding consists of only two parallel tracks positioned close to each other. But such a WG structure does not allow for control over the WG properties. On the other hand, due to geometric flexibility, the depressed cladding may consist of a fairly large number of arbitrarily arranged tracks confining the flexibly large and shaped core guiding area [16, 17]. Depressed-cladding WGs have been demonstrated to achieve light propagation with good mode confinement at different wavelengths, and low propagation losses.

The problem remaining is how to design and fabricate these, sometimes, complex buried WG structures.

2. NUMERICAL SIMULATION
In this work we modelled depressed-cladding WG structures with hexagonal symmetry, because this is a fairly commonly used WG shape, which has already been well studied in the case of isotropic materials such as MOFs. First question is how to ensure accurate simulation of depressed index cladding WGs as they often exhibit leaky-mode features [18], especially when the thickness of the cladding structure and the RI contrast between the low-index tracks of the cladding structure and the core guiding region are small. Perfectly matched layer (PML) absorber was used to minimize the effect of boundary reflections, and thus effect of mode leakage. We used COMSOL simulation software to find out the complex effective indices of both o- and e- modes of the structure (electric field directed along x and z axis). Perfectly matched layer (PML) absorber was used to truncate the computational domain and minimize the effect of boundary reflections. We chose a circular PML surrounding (20 um thick, with gradually increasing imaginary part of RI up to -0.05). Example of the Gaussian-like mode at

3 um, structure (selected using the criterium of 'minimum effective mode area'), is given in fig. 1, d, and figure (d) is to compare the actual thickness of PML and the structure diameter. The PML performance has been tested on known photonic fibres designs (isotropic case) and revealed quantitative agreement over the whole range.

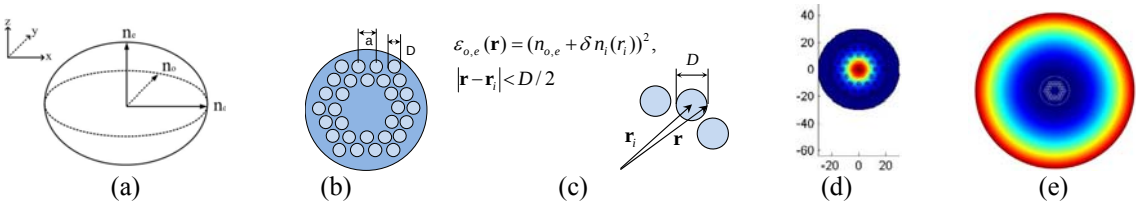

(a) (b) (c) (d) (e)

Figure 1. Ellipsoid of refractive indices (a); geometry for simulations (b); model of fs inscribed track (c), example of calculations of a Gaussian-like mode at; PML layer dimensions compared to a structure size (e).

In our initial study [19] we found that: 1) the most important parameter for managing WG structure performance is the RI contrast, other geometry parameters (period, track diameters, particular patterns play auxiliary role); 2) strong leaking of extraordinary wave (E||z) to o-wave occurs, especially at shorter wavelengths (see figs. 2 b, d); 3) with the RI contrast values experimentally achieved so far, it seems impossible to provide satisfactory loss level (1 dB/cm) even at telecom band; 4) adding additional layers with quite moderate RI contrasts of -0.01 enables to extend the operation range even beyond the telecom wavelengths range. Very complex optimisation problem has to be solved in order to benefit from the geometry. Finally, precise information about the experimentally achievable RI contrast and tracks dimensions is required.

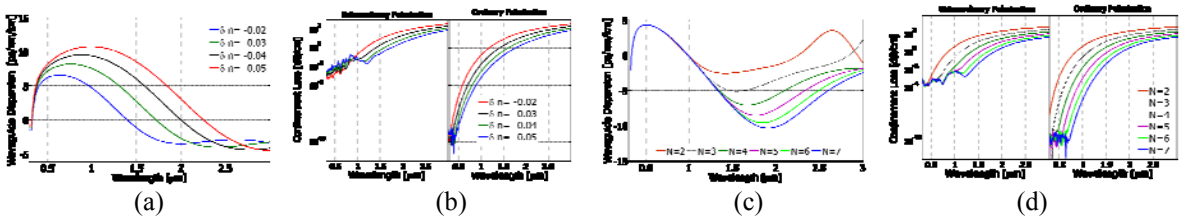

(a) (b) (c) (d)

Figure 2. Results of numerical simulations of two-ring structures with variable RI contrast (a) and its loss figures for e- and o-polarization for symmetric mode (b). The parameters in cases a-d were:…….. Dispersion and loss figures for the case of hexagonal structures with variable number of rings - plots (c) and (d) respectively. Note that each individual track in structures c), d) has refractive index contrast of -0.01. Figures adopted from [19].

3. FABRICATION OF MICROSTRUCTURED WAVEGUIDES BY DIRECT FS INSCRIPTION

In our experiment, we used fs chirped-pulse oscillator and transverse inscription geometry. Details on laser system and experimental setup and procedures can be found in [16]. In contrast to previous studies we used transform-limited pulses of 50 fs pulse duration (FWHM) with linear polarisation perpendicular to the direction of the scan. To measure RI contrast we used quantitative phase microscopy approach and in-house software for Abe inversion, assuming circular symmetry of the tracks cross sections (c.f. fig. 3, b). We report, for first time to our knowledge, smooth WGs with record high RI contrast, up to – 0.0127 in z-cut LiNBO3. Relations between track dimensions (R) and possible RI contrasts (δn) at various inscription speeds were found experimentally. The example results are given in fig.3 c, d. Despite R and δn are not completely independent, given the range of possible sample translation velocities, from 5 to 60 mm/sec, both can be effectively decoupled to realise necessary WG designs.

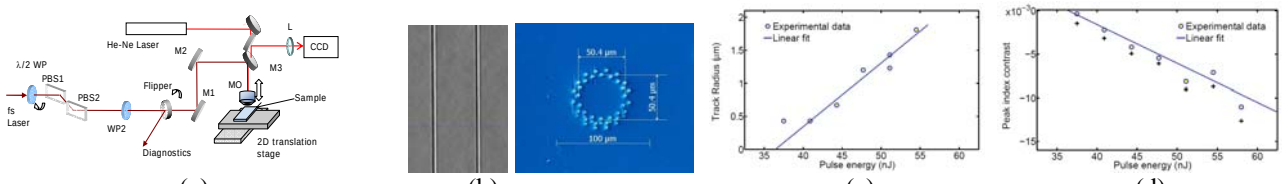

(a) (b) (c) (d)

Figure 3. Experimental setup (a), used for fabrication of microstructured waveguides in z-cut LiNbO3, and microphotograph of the waveguide and its cross-section after edge polishing (b); dependences of track dimension and induced RI contrast (c) revealed threshold-like, linear dependence which was used in numerical optimisation of the 7-ring cladding structures in next section. They were obtained with oil-immersed micro-objective lens (NA=1.25) at the depths from 250 to 400μm, at sample translation speed of 12 mm/sec.

4. OPTIMISATION RESULTS

To minimise the confinement losses in the WG structure at the long wavelengths, or, in other words, to extend the spectral range of operation, where the loss figures for the fundamental and other modes are acceptably low, we used simple idea which came from the observation that the confinement losses become monotonic functions at sufficiently long wavelengths (c.f. fig. 2 b, d). The loss at a sufficiently long wavelength can be used as a target function for optimisation. Thus, one can vary different WG structural parameters at this wavelength of interest, and only when the best loss figures are obtained, perform full wavelength scan. This makes the optimisation procedure much less time consuming and, thus, practically feasible. The growth rate of the track radius, R (which is coupled to the refractive index contrast, δn) can be parameterised by a single parameter, p as: $D_n = D_{min} + (n-1/N_{clad}-1)^p * (D_{max}-D_{min})$, n □ [1,Nclad]. The examples of 7-ring structures with p=0 (uniform structure), 0.2, 1, 5 are presented in fig. 4,a. Figure 4, b illustrates the dependence of the confinement loss at the wavelength λ = 1.55 μm on the track diameter for a seven-ring, uniform (p = 0) structure with different values of δn. It is seen that for δn=−0.01 and δn=−0.02 there is a "plateau" of low losses over the diameter range 2.2μm to 2.5μm and 1.4μm to approximately 2.2μm, respectively. Note that such plateau does not exist at lower RI contrasts in uniform structure, typical e.g. for low-repetition rate fs inscription. Such results gave us a hint on choosing the range of variations of the track diameters. Various aspects of track structural parameters were considered in a similar way. One of the parameters is the level of induced losses in fs-written tracks, whose appearance may be associated with either induced colour centres (e.g. absorption in material in or around tracks) or scattering losses. In order to understand influence of this effect one can modify the induced refractive index dependence (Fig.1,c). The results of simulations revealed that the induced losses became essential, when their value (in dB/cm) are comparable with the total WG losses, which was expected. Finally, for the optimum structure we made a wide wavelength range scan (fig 4. d) which revealed that optimised 7-ring structure, even with moderate RI contrasts, can effectively guide radiation at the wavelengths as long as 3.5μm. It is also clear that the HRR fs laser technology can be easily extended to periodically poled crystals, thereby enabling a wide spectrum of applications in classical and quantum nonlinear integrated optics.

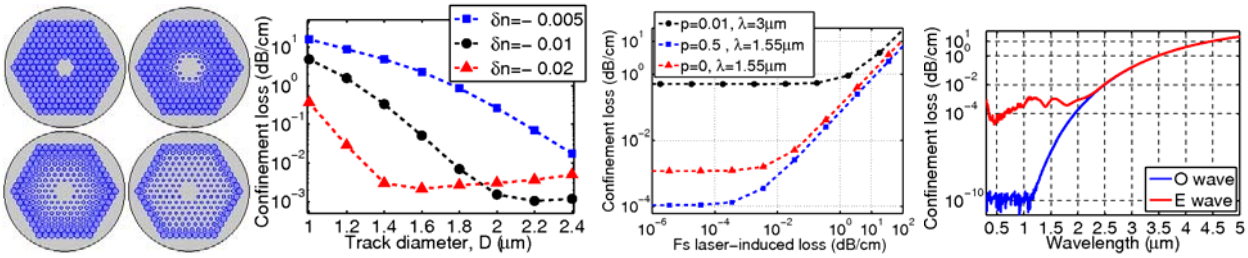

Figure 4. Example of 7-ring depressed cladding structures defined through a single parameter, p – growth rate (a);

Finally, we would like to note that the requirements on the number of tracks' rings make HRR fs laser inscription the preferred microfabrication technique. For example, for a propagation length of 10cm in a WG with seven rings (around 200 tracks) the total length of the inscribed lines would amount to approximately 20m. Clearly, if one uses a kHz fs system (with a typical sample translation speed of 10 to 100μm/s, or of 500μm/s - by use of astigmatic beam inscription [20]), the fabrication time required on a single structure can exceed 60 hours, whereas a HRR system can do the job in less than an hour.

5. CONCLUSIONS

Optimized designs of WG structures with seven cladding layers were numerically shown to achieve acceptably low (below 1dB/cm) confinement losses (i.e., losses due to the finite transverse extent of the confining structure) for both O and E polarizations over a wide spectral range, extending into the mid-infrared region up to the end of the transparency range of the host material. We have reported on the inscription regimes that are required to fabricate low-loss, microstructured, buried WGs in z-cut LiNbO3 crystals by HRR fs laser system. Record-high RI contrasts of -0.0127 have been obtained for individual modification tracks. These results offer promising means for the development of microstructured WGs in nonlinear crystals which are suitable for integrated optics applications in both the near- (telecommunications) and midinfrared spectral regions.

ACKNOWLEDGEMENTS

We acknowledge support by the Leverhulme Trust (grant RPG-278) and the Engineering and Physical Sciences Research Council (EPSRC grant EP/J010413/1).

REFERENCES

[1] M.F. T. Suhara Waveguide Nonlinear-Optic Devices, Springer-Verlag, 2003.
[2] S. Nolte, M. Will, J. Burghoff, A. Tuennermann, Femtosecond waveguide writing: a new avenue to three-dimensional integrated optics, Applied Physics a-Materials Science & Processing, 77 (2003) 109-111.
[3] R. Osellame, G. Cerullo, R.E. Ramponi, Femtosecond Laser Micromachining, 1 st ed., Springer, 2012.
[4] A.G. Okhrimchuk, A.V. Shestakov, I. Khrushchev, J. Mitchell, Depressed cladding, buried waveguide laser formed in a YAG : Nd3+ crystal by femtosecond laser writing, Optics Letters, 30 (2005) 2248-2250.
[5] A.G. Okhrimchuk, A.V. Shestakov, I. Khrushchev, I. Bennion, Waveguide laser formed in YAG : Nd3+ crystal by femtosecond laser, in: H.J. Hoffman, R.K. Shori (Eds.) Solid State Lasers XIV: Technology and Devices, Spie-Int Soc Optical Engineering, Bellingham, 2005, pp. 258-264.
[6] M. Heinrich, K. Rademaker, S. Nolte, Waveguides in Crystalline Materials, Femtosecond Laser Micromaching: Photonic and Microfluidic Devices in Transparent Materials, 123 (2012) 295-313.
[7] Y.-L. Wong, D. Furniss, V.K. Tikhorairov, E.A. Romanova, M. Dubov, T.D.P. Allsop, V. Mezentsev, I. Bennion, T.M. Benson, A.B. Seddon, Femtosecond laser writing of buried waveguides in erbium III-Doped oxyfluoride glasses and nano-glass-ceramics, in: 2008 10th Anniversary International Conference on Transparent Optical Networks, ICTON, June 22, 2008 - June 26, 2008, Inst. of Elec. and Elec. Eng. Computer Society, Athens, Greece, 2008, pp. 234-238.
[8] A. Rodenas, A. Benayas, J.R. Macdonald, J. Zhang, D.Y. Tang, D. Jaque, A.K. Kar, Direct laser writing of near-IR step-index buried channel waveguides in rare earth doped YAG, Optics Letters, 36 (2011) 3395-3397.
[9] A. Fuerbach, S. Gross, M. Ams, W. Koehler, G. Marshall, C. Miese, P. Dekker, D. Lancaster, M. Withford, Integrated Waveguide Lasers, 2011.
[10] T. Allsop, M. Dubov, V. Mezentsev, I. Bennion, Inscription and characterization of waveguides written into borosilicate glass by a high-repetition-rate femtosecond laser at 800 nm, Appl Opt, 49 (2010) 1938-1950.
[11] C.B. Schaffer, J.A.D. Au, E. Mazur, J.A. Squier, Micromachining and material change characterization using femtosecond laser oscillators, in: G.S.N.J.O.A.S.J.C. Edwards (Ed.) Commercial and Biomedical Applications of Ultrafast and Free-Electron Lasers, 2002, pp. 112-118.
[12] S.M. Eaton, P.R. Herman, Passive Photonic Devices in Glass, in: R.C.G.R.R. Osellame (Ed.) Femtosecond Laser Micromaching: Photonic and Microfluidic Devices in Transparent Materials, 2012, pp. 155-195.
[13] A. Royon, Y. Petit, G. Papon, M. Richardson, L. Canioni, Femtosecond laser induced photochemistry in materials tailored with photosensitive agents Invited, Opt. Mater. Express, 1 (2011) 866-882.
[14] K.L.N. Deepak, R. Kuladeep, S.V. Rao, D.N. Rao, Studies on defect formation in femtosecond laser-irradiated PMMA and PDMS, Radiation Effects and Defects in Solids, 167 (2012) 88-101.
[15] A.M. Streltsov, Femtosecond-laser writing of tracks with depressed refractive index in crystals, in: A. Ostendorf (Ed.) Laser Micromachining for Optoelectronic Device Fabrication, Spie-Int Soc Optical Engineering, Bellingham, 2003, pp. 51-57.
[16] H. Karakuzu, M. Dubov, S. Boscolo, L.A. Melnikov, Y.A. Mazhirina, Optimisation of microstructured waveguides in z-cut LiNbO3 crystals, Optical Materials Express, 4 (2014) 541-552.
[17] H. Karakuzu, M. Dubov, S. Boscolo, Control of the properties of micro-structured waveguides in lithium niobate crystal, Opt Express, 21 (2013) 17122-17130.
[18] J. Hu, C.R. Menyuk, Understanding leaky modes: slab waveguide revisited, Adv. Opt. Photon., 1 (2009) 58-106.
[19] H. Karakuzu, M. Dubov, S. Boscolo, Control of the properties of micro-structured waveguides in lithium niobate crystal, Optics Express, 21 (2013) 17122-17130.
[20] A.G. Okhrimchuk, V.K. Mezentsev, H. Schmitz, M. Dubov, I. Bennion, Cascaded nonlinear absorption of femtosecond laser pulses in dielectrics, Laser Physics, 19 (2009) 1415-1422.